



Research article

Microstructure and morphology of the soldering interface of Sn–2.0Ag–1.5Zn low Ag content lead-free solder ball and different substrates

Jin Xiao^{*}, Xing Tong, Jinhui Liang, Quankun Chen, Qiming Tang

Department of Mechanical and Electrical Engineering, Guangzhou Huali College, Guangzhou 511300, China



ARTICLE INFO

Keywords:

Sn–Ag–Zn
Lead-free solder
Interfacial reaction
Low silver solder
Solder joint

ABSTRACT

Eutectic Sn–Ag–Cu lead-free solder has limited applications due to cost and reliability issues. Sn–Ag–Zn solder has the advantages of low melting point, good mechanical properties and reliable welding interface. However, the research system of low silver content Sn–Ag–Zn solder is incomplete. In this paper, Sn–2.0Ag–1.5Zn low silver content alloy solder is soldered to different substrates. The interfacial reaction after soldering and the microstructure and reliability under different aging treatment conditions are studied. Sn–2.0Ag–1.5Zn solder is made into solder balls by direct melting method. The solder balls are placed in a solder strength tester to be heated and welded to the substrate, and then the solder joints are placed in a heating furnace for aging treatment. The results show that the solder is soldered to the bare Cu substrate, and a dense double-layer Intermetallic Compound (IMC) structure of Cu_5Zn_8 and Ag_3Sn is formed at the interface after aging treatment. The double-layer structure blocks each other, limiting the development of copper-tin IMCs. The solder is soldered with the Cu substrate electroplated with Ni barrier layer, and the soldering interface forms a thin layer of Ni_3Sn_4 metal compound. After aging for 1000 h, the thickness of Ni_3Sn_4 is about 1 μm , the thickness of Ni barrier layer is kept at 2–3 μm , and the barrier effect of Ni barrier layer is stable. Sn–2.0Ag–1.5Zn solder has excellent loss performance in long aging treatment. It has good heat-resistance aging treatment, good quality of solder connection, high interface reliability and less environmental pollution. The low silver content in Sn–2.0Ag–1.5Zn solder results in a significant cost reduction. Coarse IMC Ag_3Sn is not easily formed. The optimized ratio of Ag and Zn in Sn–2.0Ag–1.5Zn solder improves the strength and toughness of the solder joint. The performance has been improved, and it is a very promising alloy solder.

1. Introduction

Lead-free solder is one of the current research hotspots [1,2], developed from the fusion of microelectronics technology and environmental protection requirements. Sn–Ag based solder cannot meet the development requirements of packaging technology due to its high melting point and high cost [3–6]. In order to improve the comprehensive properties of Sn–Ag based solders, many researchers have obtained lead-free solders with excellent performance by adding other elements. Sn–Ag–Cu based and Sn–Ag–Zn based alloy solders are considered to be the most promising of lead-free solders [7–10]. Sn–Ag–Cu eutectic solder still has some problems, for

^{*} Corresponding author. Guangzhou Huali College, No. 11 Huali Rd., Zengcheng District, Guangzhou 511300, China.
E-mail address: 67104869@qq.com (J. Xiao).

<https://doi.org/10.1016/j.heliyon.2023.e12952>

Received 8 October 2022; Received in revised form 7 January 2023; Accepted 10 January 2023

Available online 13 January 2023

2405-8440/© 2023 Published by Elsevier Ltd.

This is an open access article under the CC BY-NC-ND license

(<http://creativecommons.org/licenses/by-nc-nd/4.0/>).

example, the high cost, the coarser and larger IMC and the higher melting point which greatly reduce the reliability [11–15]. [16] studied the addition of TiN nanoparticles to Sn–Ag–Cu solder and found that it significantly enhanced the wettability and mechanical properties of the solder joints. Wang et al. [17,18] studied the Sn–Ag–Cu Ternary Metal Coating Solder, they found that with the increase of Ag content, the elongation will decrease obviously, and the alloy strength will increase. This is because the number of Ag₃Sn particles will increase during the aging process, causing cracks to form along the particle interface [19] found poor thermal cycling performance and impact resistance of low silver content Sn–Ag–Cu solders. After adding Cu components to Sn–Ag–Cu solder, the comprehensive properties of all aspects have been greatly improved, but the wettability has decreased significantly high, which is quite different from Sn–Pb solder [20–22]. Solder joint reliability can be improved by adding zinc to lead-free solder. Wang et al. [17,18] found that the addition of 0.2 and 0.4 wt% Zn significantly inhibited the growth of IMC thickness in Sn-10 Bi/Cu solder joints during aging [23] studied the microstructure changes after adding a small amount of Ag to Sn–9Zn solder, which improved the toughness of the solder alloy [24] found that with the increase of Ag content in Sn–9Zn solder, the melting point and melting range of the solder increased, and Zn combined with the Intermetallic Compound (IMC) formed with the corrosion-resistant element Ag can improve the corrosion resistance of the solder. The addition of the third element Zn to Sn–Ag based solders is less studied, and Sn–Ag–Zn based solders with low silver content are the current research focus. Xiong and Zhang [25] found that Sn–3.5Ag–2Zn alloy solder has high strength, but poor plasticity compared with Sn–Ag–Cu based solder. Element Zn inhibits the growth of IMC at the solder joint interface and improves the reliability of the solder joint interface connection. Low silver content Sn–Ag–Zn solder has low melting point, good mechanical properties, good reliability of solder joint interface, and Zn has strong metallicity and good toughness, which ensures the mechanical properties of solder. There are few reports, and it has great development prospects [26–28].

The objective of this paper is to address the reduction in wettability and mechanical properties caused by the reduced silver content in low silver solders. According to the wetting properties of Sn–Ag–Zn solder, an optimal proportion of solder Sn–2.0Ag–1.5Zn was selected, and Sn–2.0Ag–1.5Zn alloy solder was soldered with electroplated nickel barrier copper substrates and bare copper substrates, the interface structure of the solder joint and the interface structure at 220 °C at different aging treatment time were analyzed, and the types and properties of the IMCs at the solder joint were analyzed. Sn–2.0Ag–1.5Zn/Cu solder joints have good strength and toughness. However, severe interfacial reactions occur after prolonged aging. Solve the problem of interfacial brittleness of solder joints by plating Ni with copper solder pans. Sn–2.0Ag–1.5Zn/Ni/Cu solder joints have good toughness and excellent loss performance in long aging treatment.

2. Experiment

Pure tin (Sn), pure zinc (Zn) and pure silver (Ag) were added into the crucible by mass ratio and melted. The temperature was set to 600 °C, and the time was set to 30 min. The raw materials used are shown in Table 1. The metal surface in molten state was covered with KCl–LiCl and stirred well to obtain a homogeneous Sn–Ag–Zn alloy. 1 g of the alloy was weighed and melted into the rosin solution, and the heating temperature of the rosin solution was set to 260 °C. After the solder was melted, it is formed into a spherical shape under the action of surface tension. Diameter of the solder ball is about 0.8 mm. After the solder ball was formed, it was cooled in quenching oil, washed with acetone, and dried for storage.

Solder spreading test was conducted with reference to China national standard GB11364-89. A copper plate with a size of 150 mm × 150 mm was rinsed with deionized water after degreasing, and then corroded in 10% HCl for 10 s to remove the oxide film, rinsed with deionized water, and dried. 1 g of solder ball was placed on a copper plate, and then placed on a hot plate for 180 s. The temperature of the hot plate was set to 260 °C. After waiting for the solder to cool, measure its the area of solder spread and take the average of 3 data for each alloy solder.

Take a bare copper substrate with a size of 50 mm × 50 mm and a copper substrate with an electroplated Ni barrier layer, and use a Rhesca PTR-1102 soldering strength tester with a heating plate to conduct soldering experiments. The substrate was fixed on a heating plate and heated to 220 °C, and the prepared alloy solder balls were dipped in flux and placed on the substrate. The soldering time was set to 30 s to make the solder fully spread. The schematic diagram of copper substrate soldering with Ni barrier layer is shown in Fig. 1. After the soldering was completed, the substrate was left to cool at room temperature. The solder joints soldered to the surfaces of different substrates were placed in a heating furnace at 220 °C for aging for 10, 100, and 1000 h, respectively.

The residual solder at the solder joint was polished to 1 μm with sandpaper, and the remaining solder was removed by etching with 10% HNO₃ to expose the metal compound at the cross-section. Secondary electron imaging (SE) and backscattered electron imaging (BSE) with a scanning electron microscope (SU8220, Hitachi, JAPAN), energy dispersive spectrometer (INCA OXFORD), Rigaku D/MAX-III A X-ray polycrystalline diffractometer (The target Cu Kα, λ = 0.15418 nm) were used to characterize the morphology and quantitatively analyzed the microstructure of the solder joint interface after reflow soldering and aging treatment. The samples of secondary electron imaging were etched with a volume fraction of 2% HNO₃ after polishing, and the backscattered electron samples were not etched after polishing.

Table 1
Physical data of raw materials.

Element	Atomic number	Melting point (°C)	Density (g/cm ³)	Material shape	Purity	Manufacturer
Sn	50	231.9	7.298	Ingot casting	4 N	Yunnan Tin Group
Zn	30	419.6	7.134	Granular	3.5 N	Sinopharm
Ag	47	961	10.5	Flakes	4 N	Sinopharm

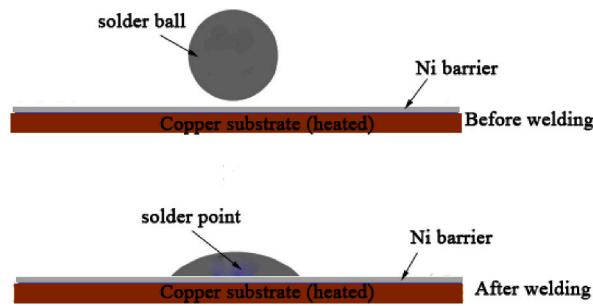


Fig. 1. Soldering diagram of copper substrate plated with Ni barrier layer.

3. Test results and discussions

3.1. Sn–Ag–Zn alloy solder wettability

The wettability of the solder alloy is evaluated by measuring the solder ball spreading area. Fig. 2 shows the test results of the spreading area of the Sn–Ag–Zn alloy solder with low Ag content. It is found that the content (mass fraction) of Ag in the Sn–Ag–Zn solder has great influence on the wettability. The wettability maintains a decreasing trend with the decrease of Ag. When the Ag content is 3%, the wettability of the solder is good and stable, and the spreading area of the solder is comparable to the commercial solder SAC105. When the Ag content decreases to 2%, the wettability of the solder decreases sharply. After the Zn content exceeds 1.5%, with the increase of Zn content, the surface tension of the solder melt increases and the increase of Zn oxide results in a decrease in wettability. However, when the Zn content is 1.0%–1.5%, the wettability increases to a certain extent with the increase of Zn content, which is because the increase of Zn content reduces the liquidus temperature and the surface tension. When the Ag content is 1%, the wettability of the Zn content of 1%–1.5% is better, and the Zn content is lower than that of the commonly used Sn–Zn solder, but the melting point of the sample is increased, which is not conducive to the wetting effect. Although low Ag content deteriorates the wettability of Sn–Ag–Zn solder, low Ag content lowers the melting point of the solder, making it difficult to form coarse IMCs. The slight addition of Zn element can reduce the surface tension of tin-based solder and improve the wettability. Zn has good toughness, excellent mechanical properties, and can inhibit the growth of IMCs at the soldering interface. Considering the melting properties, the optimal solder composition Sn–2.0Ag–1.5Zn solder is selected.

3.2. Interface morphology of Solder and optical copper substrate

Fig. 3 the microstructure of Sn–2.0Ag–1.5Zn alloy solder soldered to bare copper substrate for 30 s at 220 °C is shown. In Fig. 3(a), a layer of uniform IMC is formed between the Sn–2.0Ag–1.5Zn solder and the bare copper substrate after soldering, with a thickness of about 2 μm and good flatness. Further from Fig. 3(b), it is found that it is not a single IMC, but a complex IMC layer. The energy spectrum analysis of the AB line segment in Fig. 3(b) (Fig. 3(c)) found that Cu, Ag, Sn, Zn elements all exist at the interface, and higher at the interface of Zn and Ag elements, The content of Cu and Sn elements is low. In Fig. 3(d), XRD analysis was used to analyze the IMCs at the interface, and the IMCs contained in the interface were Ag₃Sn, AgZn₃, and Cu₅Zn₈. Among them, the IMC mixed with Ag₃Sn and AgZn₃ is on the side near the solder, the contrast is relatively shallow, and there is a tendency to advance to the inside of the solder.

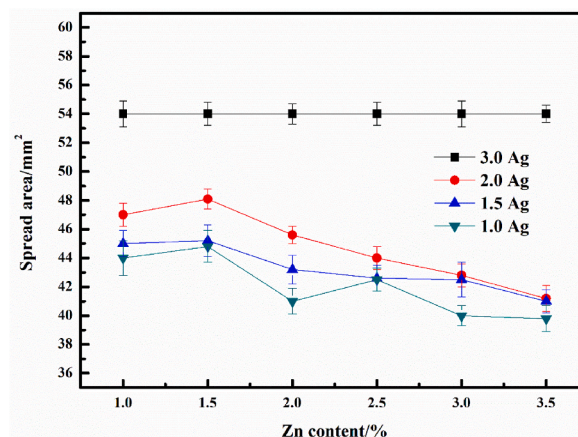


Fig. 2. Wettability of low silver Sn–Ag–Zn solder.

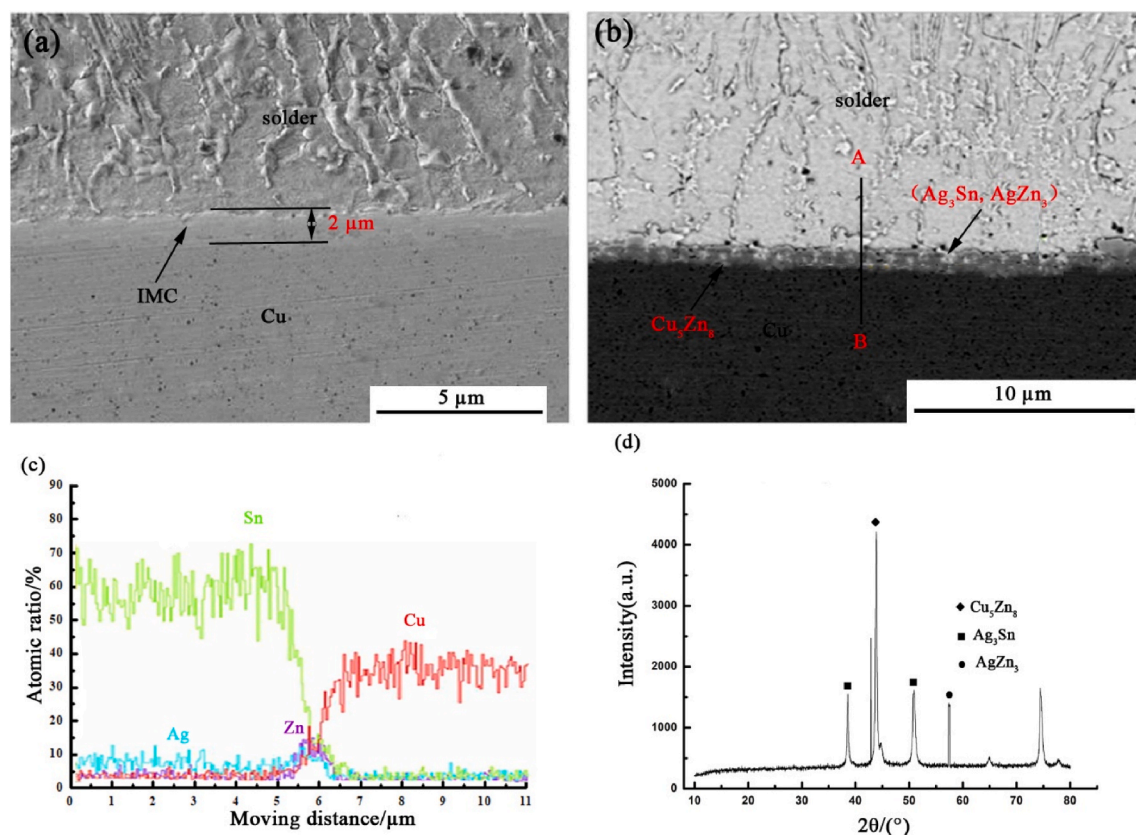


Fig. 3. Interface morphology between solder and light copper substrate: (a) secondary electron image; (b) backscattered electron image; (c) energy dispersive spectrum analysis; (d) XRD pattern.

The contrast of Cu_5Zn_8 is deep, and it is on the side close to the Cu substrate.

3.3. Solder and light copper substrate solder joint reliability

The cross-sectional morphology of the interface in contact with the solder joint after aging for 10 h is shown in Fig. 4(a). Compared with the morphology of the just-welded interface in Fig. 2, the welded interface after aging treatment for 10 h has a very prominent delamination phenomenon. Ag_3Sn pushes the extension into the solder. This single-layer structure after soldering will evolve into a layered structure. The line scan analysis of the soldering interface is carried out, as shown in Fig. 4(b). Since other elements are not enriched near the interface, it is concluded that there are no other kinds of IMCs at the interface. The secondary electron morphology was observed on the top-view interface of the solder joint, as shown in Fig. 4(c). According to the results of EDX analysis in Table 2, It was found that the prominent secondary phase particles Ag_3Sn are evenly distributed, and there was a layer of flat IMC Cu_5Zn_8 below the granular Ag_3Sn .

Aging treatment extended time to 100 and 1000 h, respectively, and the interface morphology is shown in Fig. 5. After 100 h, the interface morphology further evolves on the double-layer structure in Fig. 5(a). A bilayer structure covering this interface is formed. The amount of Ag_3Sn with lower contrast increases, and the coverage area continues to increase. In Fig. 5(b), The volume and number of granular Ag_3Sn increased after aging for 100 h. In Fig. 5(d), after 1000 h of aging treatment, Ag_3Sn basically covered the entire interface. Ag_3Sn completely covered the Cu_5Zn_8 at the bottom, but the thickness increment of Ag_3Sn was very small and remained around 4 μm . With the increase of aging, the morphology of Cu_5Zn_8 basically does not change, the flatness and thickness are relatively stable. The Ag_3Sn and Cu_5Zn_8 composed two-layer structure which producing a similar effect as a barrier layer. As shown in Fig. 5(c), The morphologies of the IMCs are obviously different when the aging treatment time reaches 1000 h Ag_3Sn continuously penetrates toward the inside of the solder, separates from Cu_5Zn_8 , and its density becomes significantly thinner. Decomposition of Cu_5Zn_8 produces a new intermetallic product Cu_6Sn_5 , which is 6 μm thick. Both the separation of Ag_3Sn and Cu_5Zn_8 can be clearly observed, and the newly combined copper-tin compound can be seen. The boundary of the IMC at the interface of the solder joint is not obvious, which is due to the diffusion of Cu element to form a dispersed IMC.

Table 3 is a statistical table of the thickness of IMCs (IMC) of each phase obtained by selecting 9 samples from each group and taking the average value under different heat treatment conditions. It is speculated that the thickness of the IMCs (Ag_3Sn , Cu_6Sn_5) at the soldering interface is relatively stable at about 11 μm after long-aging treatment.

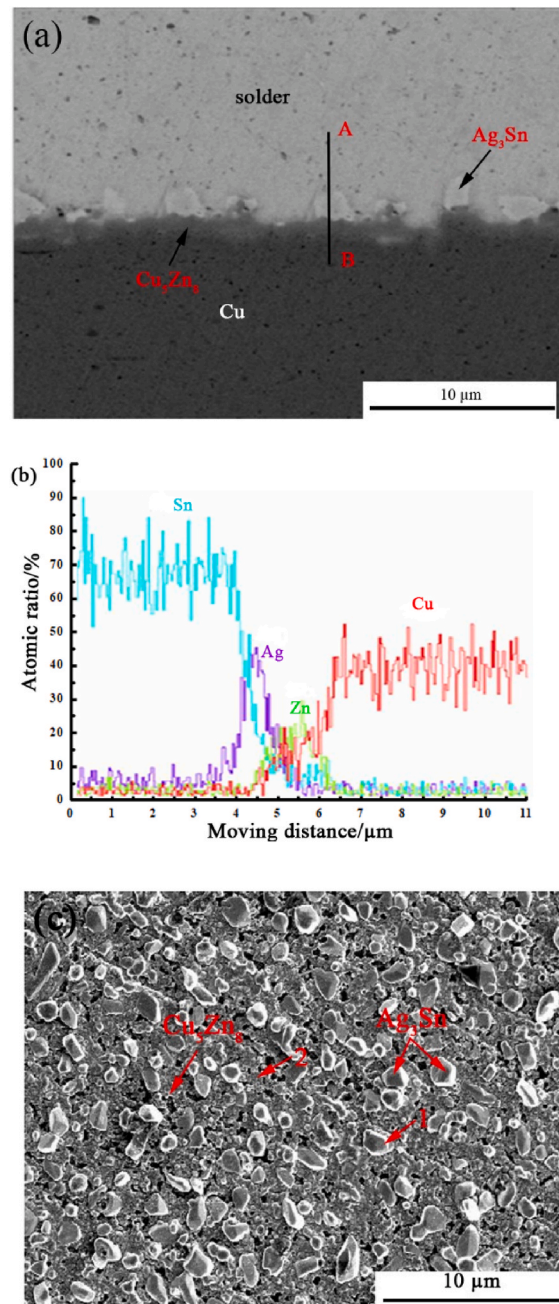


Fig. 4. The interface morphology of the solder-bonded light copper substrate after aging for 10 h: (a) backscattered electron image; (b) energy spectrum line scanning analysis; (c) secondary electron morphology of solder joint from top view.

Fig. 6 shows the thickness of interfacial IMCs of solder and Cu solder joints as a function of aging time. The IMC gradually thickens with increasing aging time. The decrease in the increase of Cu–Zn IMC thickness after 100 h of aging is due to the decomposition of Cu_5Zn_8 at high temperature. The Ag_3Sn thickness increases slowly and is obviously inhibited by the Cu_5Zn_8 below. The interfacial IMC growth rate is calculated from the linear law [29–31] to be about $2.3 \times 10^{-18} \text{ m}^2/\text{s}$. The increase in the interfacial Cu–Sn or Cu–Zn IMC growth rate is much smaller compared to that of Sn–Ag–Cu solder or Sn–Zn solder [32–34]. This indicates that the double-layer IMC formed by the solder and the Cu substrate inhibit each other's growth. The possibility of failure of the solder joint interface due to thickening of the brittle IMC with reduced flatness is reduced.

Calibrated by XRD for compounds on the interface surface. As shown in Fig. 7, the IMCs mainly include Ag_3Sn , Cu_6Sn_5 , with Cu_5Zn_8 . This result is consistent with that obtained using energy spectroscopy to analyze elemental content.

As shown in Fig. 8(a), after completing the aging treatment for 1000 h, the etch pit morphology appeared at the interface in some

Table 2
EDX analysis results in Fig. 4(c).

Location	Element	Atomic percentage/%
1 point	Cu	28.73
	Zn	24.63
	Ag	30.43
	Sn	16.21
2 point	Cu	36.56
	Zn	58.09
	Ag	4.23
	Sn	1.12

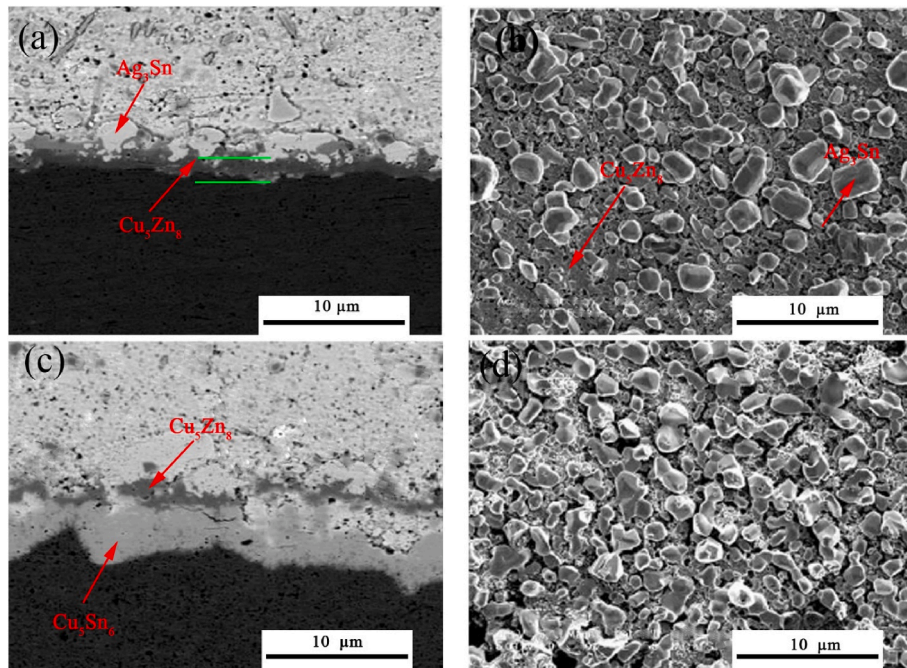


Fig. 5. Morphology of bare copper substrate and solder: (a) backscattered electron image of interface morphology after aging treatment time reaches 100 h; (b) secondary electron morphology of solder joint from top view after aging for 100 h; (c) backscattered electron image of interface morphology after aging for 1000 h; (d) secondary electron morphology of solder joint from top view after aging for 1000 h.

Table 3
Statistical table of IMC thickness of each phase after different aging treatments.

Aging time/h	IMC	Average thickness/ μm
0	IMC(Ag ₃ Sn, AgZn ₃ , Cu ₅ Zn ₈)	2.033
10	Ag ₃ Sn	1.989
	Cu ₅ Zn ₈	2.012
	Ag ₃ Sn	3.245
100	Ag ₃ Sn	3.245
	Cu ₅ Zn ₈	3.435
	Ag ₃ Sn	4.011
1000	Ag ₃ Sn	4.011
	Cu ₅ Zn ₈	1.078
	Cu ₅ Sn ₆	5.992

areas. Where the alloyed solder is bonded to the Cu substrate, islands of Ag₃Sn are located within the Sn-rich structure, while Cu₆Sn₅ is dispersed around the Ag₃Sn. Below the interface, the tin in the solder reacts with the copper substrate to form IMCs of copper and tin. In Fig. 8(b), the dotted island-shaped erosion pit is the initial contact position between the solder and the copper substrate. Sn erodes to the depth of the earliest contact interface, forming a copper-tin IMC below the original interface. After removing the easily corroded Sn solder, two points were taken at the bottom of the erosion pit for elemental analysis, as shown in Table 4. It can be seen that the content of Zn and Ag at the bottom of the cavity is relatively low, The copper-tin IMC formed by Sn atoms and Cu atoms according to the composition ratio should be Cu₆Sn₅.

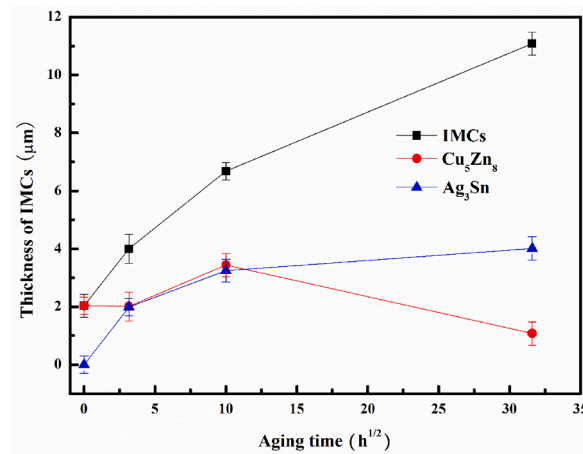


Fig. 6. Variation of IMCs thickness at Sn-2Ag-1.5Zn solder/Cu substrate interface with aging time at 220 °C.

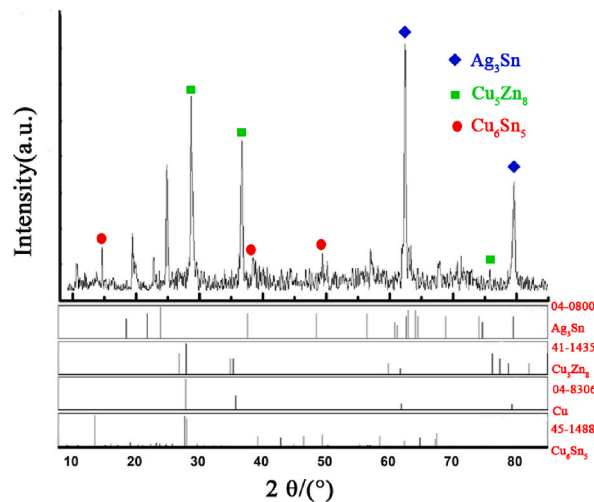


Fig. 7. XRD pattern of interface between solder and copper substrate.

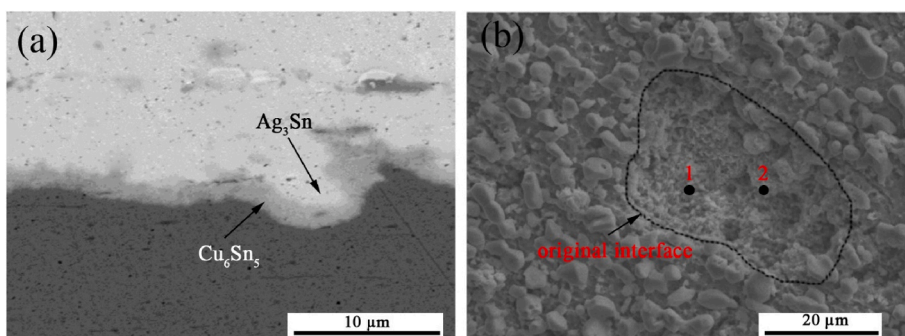


Fig. 8. Corrosion pits of solder and copper substrates at the interface: (a) Interfacial distribution morphology. (b) Top view morphology.

3.4. Solder connection to copper substrate electroplated with Ni barrier layer

Sn-2.0Ag-1.5Zn solder was aged at 220 °C for a long time, which will corrode the copper substrate. Ni plating was used to solve the problem of solder corrosion. Fig. 9(a) shows the surface of the electroplated Ni barrier layer with excellent surface flatness and density.

Table 4
Scanning analysis results of corrosion pits at bottom points.

Location	Element	Atomic percentage/%
1 point	Cu	52.20
	Zn	8.50
	Ag	1.62
	Sn	37.68
2 point	Cu	50.13
	Zn	7.96
	Ag	1.73
	Sn	40.18

Fig. 9(b) shows the cross-sectional morphology of the interface between Sn–2.0Ag–1.5Zn alloy solder and the substrate plated with Ni barrier layer after soldering for 30 s at 220 °C. The thickness of the Ni layer is 4 μm. The upper and lower sides of the Ni barrier layer are solder and copper substrates, respectively, and no IMCs are formed, it shows that the Ni barrier material has excellent barrier effect. Fig. 9(c) is the line scan analysis result of the tissue at line AB in Fig. 8(b). There is no enrichment of Sn, Zn, Ag and other elements in the interface area between the solder and the Ni layer. There is no IMC formed at the interface between the Ni barrier layer, the Cu substrate and the solder.

Sn–2.0Ag–1.5Zn alloy solder balls were soldered on Cu substrates plated with Ni layer barrier. When the aging treatment reaches 10 h at 220 °C, the shape of the weld is shown in Fig. 10(a). The alloy solder and the nickel barrier layer form the IMC Ni₃Sn₄. As the aging time increases, the thickness of Ni₃Sn₄ becomes slightly thicker. The thickness of the barrier layer was reduced, but the soldering interface layer did not thicken, and the barrier effect was excellent. The nickel atoms did not diffuse to either side of the interface. The matrix Cu atoms and the alloying elements Zn, Sn, and Ag in the solder stop at the barrier isolation layer continue to diffuse. Although the content of Zn element in the solder is 2.5%, there is no obvious aggregation of Zn element at the interface of the solder joint, and Sn, Ni and Ag are uniformly distributed at the interface of the solder joint. As shown in Fig. 10(b)–(d), the aging treatment time was extended to 1000 h, and the microstructure of the interface was observed after 240, 480 and 1000 h, respectively. We found through research that the thickness of the IMC Ni₃Sn₄, which acts to connect the barrier spacer and the solder balls, increases with the prolonging of the aging treatment time. Because the barrier layer grows more slowly, its thickness is also reduced. This can be thought of as the behavior of the reaction at consuming the barrier interface. The thickness of the barrier layer remained around 2–3 μm after 1000 h of aging treatment at 220 °C. The blocking effect, morphology and state of the Ni blocking layer are basically stable, and there is no reaction to other IMCs. It is presumed that after further prolonging the aging treatment time, there is no accumulation of alloying elements near the barrier layer. No other IMCs are formed, and each alloying element is uniformly distributed in the solder joint. The barrier layer effectively blocks the interface reaction between the alloy solder and the Cu substrate, and the interface morphology is relatively stable.

According to the relevant literature [25,35], when the Sn–Ag–Cu solder and the copper substrate coated with Ni barrier layer are aged at 250 °C for 4 h, the formation of granular Cu₆Sn₅ IMC will spread to the entire interior of the solder, producing the phenomenon of the solder dissolving most of the substrate.

Scanning electron microscopy was used to observe IMCs on the interface surface after etching away the solder. Shown in Fig. 11(a) is the morphology of its interface after an aging treatment time of 1000 h. A granular IMC Ag₃Sn at the interface can be observed. The particulate compound above the barrier-coated copper plate interface was less than more particulate than the bare copper substrate interface. The IMC Ag₃Sn produced during the aging treatment should be formed by the diffusion of internal elements in the metal solder. The amount of Ag₃Sn at the interface of the substrate coated with the Ni barrier layer is small. It is speculated that the formation of Ag₃Sn metal compounds is inhibited to some extent due to the formation of Ni₃Sn₄, which consumes Sn atoms, above the barrier layer.

In some positions of the top view of the interface after removing the solder, it is found that there is a phenomenon of lamellar shedding of the organization. Fig. 11(b) is the energy spectrum data of point 1. By testing the element content magnitude and distribution state, it is known that the main elements in the structure below the interface are Sn and Ni. Combined with the ratio of atomic numbers, the Ni₃Sn₄ layer has a relatively flat structure with a very low content of other metallic elements. Fig. 11(c) is the energy spectrum data of the point 2 region selected from the region after the exfoliation of the lamellar tissue. The detected elements are mainly Ni and Cu, and the good isolation effect of Ni isolation layer is further reflected. From the above, it can be inferred that the top of the layered structure is Ni₃Sn₄, and the bottom is the Ni isolation layer. The isolation layer effectively inhibits the growth of the interfacial layer and prevents the interpenetration of atoms in the Sn–2Ag–2.5Sn alloy solder and the copper substrate. Thus, further erosion of the copper substrate by the alloy solder is prevented.

4. Conclusion

4.1. Based on the results and discussions presented above, the conclusions are obtained as below

Sn–2.0Ag–1.5Zn has good wetting performance and forms complex IMCs at the interface between solder and the bare copper substrate. The interface starts to appear as a multi-layered structured IMC in the early stage of aging at 220 °C and forms Cu₅Zn₈ and Ag₃Sn sequentially along the soldering direction. A two-layer IMC structure with good flatness covering the interface is formed after

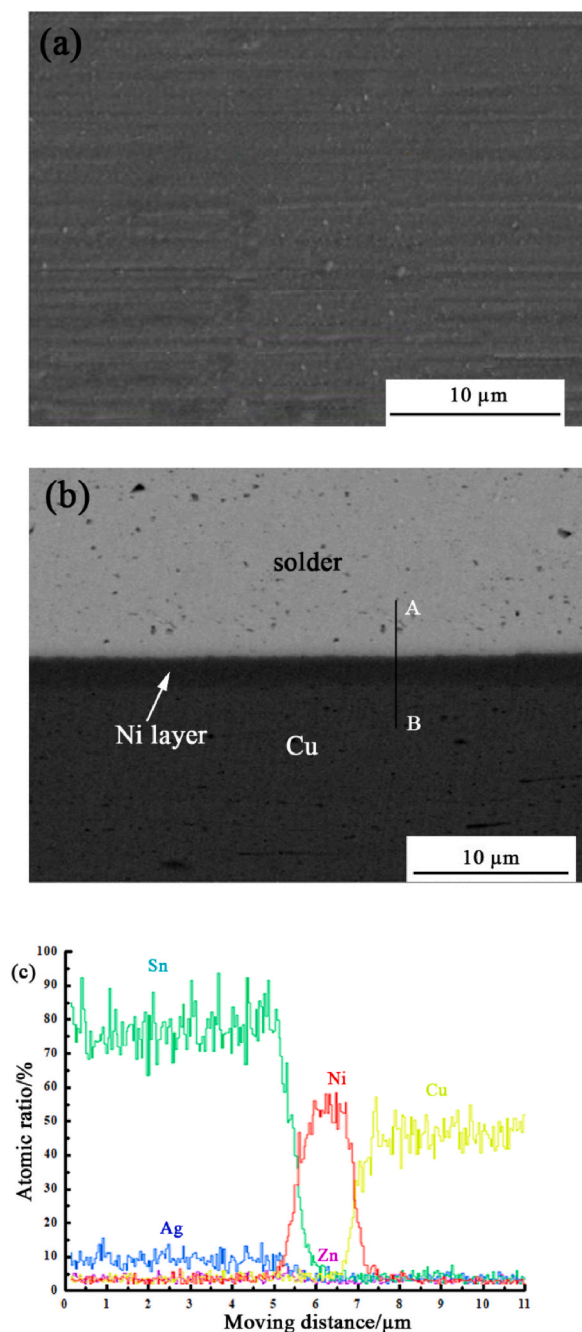


Fig. 9. Morphology of solder and Ni plated barrier layer: (a) surface of Ni plated layer; (b) interface morphology; (c) energy spectrum line scanning analysis.

the aging time is extended to 100 h. These two layers form a barrier-like effect. The interface between Sn–2.0Ag–1.5Zn alloy solder and Cu substrate coated with the Ni separator layer forms Ni_3Sn_4 . The thickness of the Ni_3Sn_4 increases slowly during aging treatment. Ni_3Sn_4 with a thickness of about 1 μm has a relatively flat surface after an aging treatment time of more than 1000 h. The nickel separator layer is stable and has ideal result of loss in long-term aging process. The low Ag content in the Sn–2Ag–1.5Zn solder results in a significant cost reduction and improved performance, making it a very promising alloy solder for application.

Author contribution statement

Jin Xiao: Conceived and designed the experiments; Analyzed and interpreted the data; Contributed reagents, materials, analysis

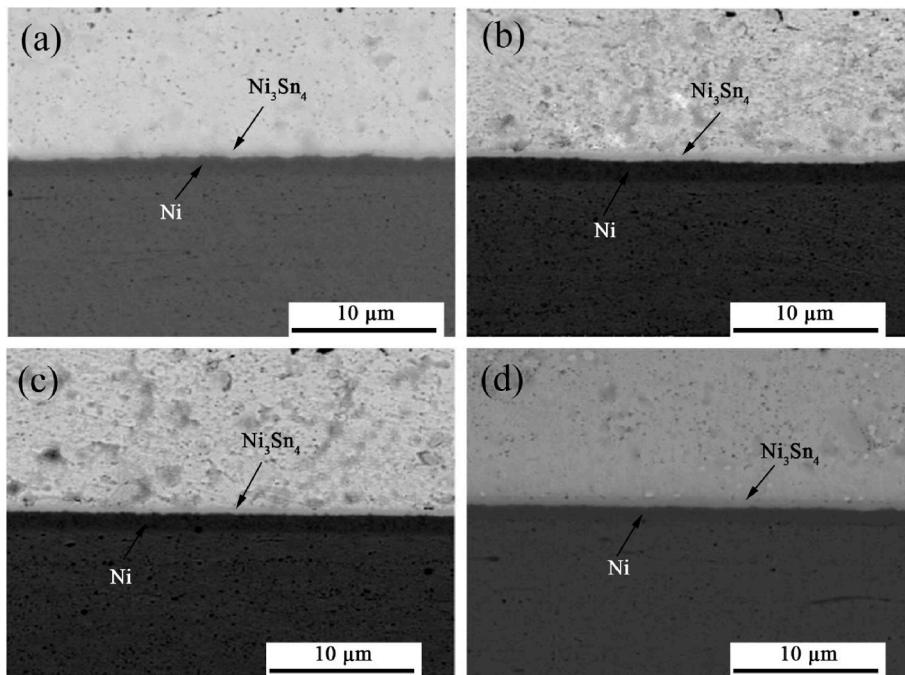


Fig. 10. Surface morphology between nickel-plated barrier substrate and solder after aging: (a) aging for 10 h; (b) aging for 240 h; (c) aging for 480 h; (d) aging for 1000 h.

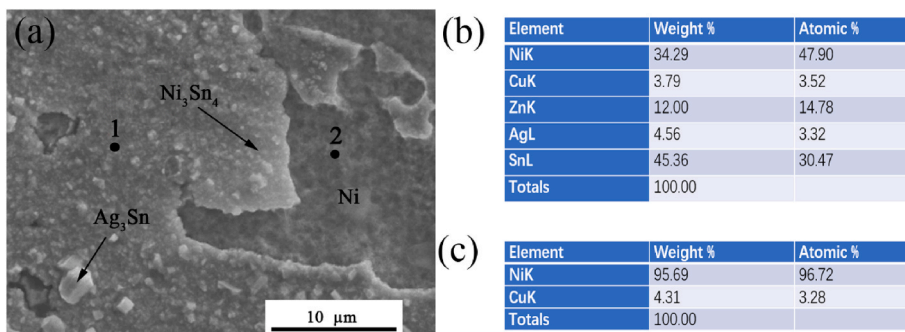


Fig. 11. Top view of the interface between solder and Ni-plated barrier substrate after aging for 1000 h: (a) interface morphology; (b) area 1 point EDS analysis; (c) area 2 point EDS analysis.

tools or data; Wrote the paper.

Xing Tong: Performed the experiments; Wrote the paper.

Jinhui Liang, Quankun Chen, Qiming Tang: Performed the experiments.

Funding statement

This work was supported by the 2021 Guangzhou Science and Technology Plan Basic and Applied Basic Research Project (NO:202102080571), Zengcheng District Science and Technology Planning Project (NO:2021ZCMS11).

Data availability statement

Data included in article/supplementary material/referenced in article.

Declaration of interest’s statement

The authors declare no competing interests.

References

- [1] E.Y. Seo, J.E. Ryu, Influence of reflow profile on thermal fatigue behaviors of solder ball joints, *J. Mater. Eng. Perform.* 29 (6) (2020) 4095–4104, <https://doi.org/10.1007/s11665-020-04899-3>.
- [2] L. Yang, S. Ma, G. Mu, Improvements of microstructure and hardness of lead-free solders doped with Mo nanoparticles, *Mater. Lett.* 304 (2021), 130654, <https://doi.org/10.1016/j.matlet.2021.130654>.
- [3] D. Soares, H. Leitão, C.S. Lau, J.C. Teixeira, L. Ribas, R. Alves, S. Teixeira, M.F. Cerqueira, F. Macedo, Effect of the soldering atmosphere on the wettability between Sn_{4.0}Ag_{0.5}Cu (in wt.%) lead-free solder paste and various substrates, *J. Mater. Eng. Perform.* 27 (10) (2018) 5011–5017, <https://doi.org/10.1007/s11665-018-3419-2>.
- [4] M. Yamamoto, I. Shohji, T. Kobayashi, K. Mitsui, H. Watanabe, Effect of small amount of Ni addition on microstructure and fatigue properties of Sn-Sb-Ag lead-free solder, *Materials* 14 (14) (2021), <https://doi.org/10.3390/ma14143799>.
- [5] R. Shalaby, M.K. Kamal, E. Ali, M. Gumaan, Microstructural and mechanical characterization of melt spun process Sn-3.5Ag and Sn-3.5Ag-xCu lead-free solders for low cost electronic assembly, *Mater. Sci. Eng., A* 690 (2017), <https://doi.org/10.1016/j.msea.2017.03.022>.
- [6] L. Xu, X. Chen, H. Jing, L. Wang, J. Wei, Y. Han, Design and performance of Ag nanoparticle-modified graphene/SnAgCu lead-free solders, *Mater. Sci. Eng., A* 667 (2016) 87–96, <https://doi.org/10.1016/j.msea.2016.04.084>.
- [7] A.A. El-Daly, A.E. Hammad, G.S. Al-Ganainy, M. Ragab, Properties enhancement of low Ag-content Sn-Ag-Cu lead-free solders containing small amount of Zn, *J. Alloys Compd.* 614 (2014) 20–28, <https://doi.org/10.1016/j.jallcom.2014.06.009>.
- [8] T. Gancarz, J. Pstrus, Formation and growth of intermetallic phases at the interface in the Cu/Sn-Zn-Ag-Cu/Cu joints, *J. Alloys Compd.* 647 (2015) 844–856, <https://doi.org/10.1016/j.jallcom.2015.06.122>.
- [9] R.M. Shalaby, M. Kamal, E.A.M. Ali, M.S. Gumaan, Design and properties of new lead-free solder joints using Sn-3.5Ag-Cu solder, *Silicon* 10 (5) (2018) 1861–1871, <https://doi.org/10.1007/s12633-017-9690-2>.
- [10] M.S. Gumaan, Chromium improvements on the mechanical performance of a rapidly solidified eutectic Sn-Ag alloy, *J. Mater. Sci. Mater. Electron.* 31 (13) (2020) 10731–10737, <https://doi.org/10.1007/s10854-020-03623-0>.
- [11] D. Soares, M. Sarmiento, D. Barros, H. Peixoto, H. Figueiredo, R. Alves, I. Delgado, J.C. Teixeira, F. Cerqueira, The effect of Bi addition on the electrical and microstructural properties of SAC405 soldered structure, *Solder. Surf. Mt. Technol.* 33 (1) (2021) 19–25, <https://doi.org/10.1108/SSMT-10-2019-0029>.
- [12] Q.K. Zhang, F.Q. Hu, Z.L. Song, Z.F. Zhang, Viscoplastic creep and microstructure evolution of Sn-based lead-free solders at low strain, *Mater. Sci. Eng., A* 701 (2017) 187–195, <https://doi.org/10.1016/j.msea.2017.06.083>.
- [13] T. Gu, V.S. Tong, C.M. Gourlay, T.B. Britton, In-situ study of creep in Sn-3Ag-0.5Cu solder, *Acta Mater.* 196 (2020) 31–43, <https://doi.org/10.1016/j.actamat.2020.06.013>.
- [14] D. Herkommer, M. Reid, J. Punch, In situ optical creep observation of joint-scale tin-silver-copper solder shear samples, *J. Electron. Mater.* 38 (10) (2009) 2085–2095, <https://doi.org/10.1007/s11664-009-0885-1>.
- [15] L. Yin, Z. Zhang, C. Zuo, N. Fang, Z. Yao, Z. Su, Microstructures and properties of Sn-0.3Ag-0.7Cu solder doped with graphene nanosheets, *J. Mater. Sci. Mater. Electron.* 31 (3) (2020) 1861–1867, <https://doi.org/10.1007/s10854-019-02705-y>.
- [16] L. Sun, L. Zhang, Y. Zhang, Y.-x. Xu, P.-x. Zhang, Q.-h. Liu, H.-j. Shan, Interfacial reaction and properties of Sn_{0.3}Ag_{0.7}Cu containing nano-TiN solder joints, *J. Mater. Sci. Mater. Electron.* 33 (6) (2022) 3320–3330, <https://doi.org/10.1007/s10854-021-07532-8>.
- [17] Q. Wang, H. Chen, F. Wang, Effect of trace Zn addition on interfacial evolution in Sn-10Bi/Cu solder joints during aging condition, *Materials* 12 (24) (2019), <https://doi.org/10.3390/ma12244240>.
- [18] Z. Wang, Q.K. Zhang, Y.X. Chen, Z.L. Song, Influences of Ag and in alloying on Sn-Bi eutectic solder and SnBi/Cu solder joints, *J. Mater. Sci. Mater. Electron.* 30 (20) (2019) 18524–18538, <https://doi.org/10.1007/s10854-019-02206-y>.
- [19] D. Abdul Ameer Shanawah, M. Faizul Bin Mohd Sabri, I. Anjum Badruddin, S. Said, A review on effect of minor alloying elements on thermal cycling and drop impact reliability of low-Ag Sn-Ag-Cu solder joints, *Microelectron. Int.* 29 (1) (2012) 47–57, <https://doi.org/10.1108/13565361211219202>.
- [20] Y. Qiao, H. Ma, F. Yu, N. Zhao, Quasi-in-situ observation on diffusion anisotropy dominated asymmetrical growth of Cu-Sn IMCs under temperature gradient, *Acta Mater.* 217 (2021), 117168, <https://doi.org/10.1016/j.actamat.2021.117168>.
- [21] H. Wang, X. Hu, X. Jiang, Effects of Ni modified MWCNTs on the microstructural evolution and shear strength of Sn-3.0Ag-0.5Cu composite solder joints, *Mater. Char.* 163 (2020), 110287, <https://doi.org/10.1016/j.matchar.2020.110287>.
- [22] X. Bi, X. Hu, Q. Li, Effect of Co addition into Ni film on shear strength of solder/Ni/Cu system: experimental and theoretical investigations, *Mater. Sci. Eng., A* 788 (2020), 139589, <https://doi.org/10.1016/j.msea.2020.139589>.
- [23] A.K. Gain, L. Zhang, Effect of Ag nanoparticles on microstructure, damping property and hardness of low melting point eutectic tin-bismuth solder, *J. Mater. Sci. Mater. Electron.* 28 (20) (2017) 15718–15730, <https://doi.org/10.1007/s10854-017-7465-6>.
- [24] M.M. Billah, K.M. Shorowordi, A. Sharif, Effect of micron size Ni particle addition in Sn-8Zn-3Bi lead-free solder alloy on the microstructure, thermal and mechanical properties, *J. Alloys Compd.* 585 (2014) 32–39, <https://doi.org/10.1016/j.jallcom.2013.09.131>.
- [25] M.-y. Xiong, L. Zhang, Interface reaction and intermetallic compound growth behavior of Sn-Ag-Cu lead-free solder joints on different substrates in electronic packaging, *J. Mater. Sci.* 54 (2) (2019) 1741–1768, <https://doi.org/10.1007/s10853-018-2907-y>.
- [26] W.-Y. Chen, R.-W. Song, J.-G. Duh, Grain structure modification of Cu-Sn IMCs by applying Cu-Zn UBM on transient liquid-phase bonding in novel 3D-IC technologies, *Intermetallics* 85 (2017) 170–175, <https://doi.org/10.1016/j.intermet.2017.02.021>.
- [27] R. Mayappan, I. Yahya, N.A.A. Ghani, H.A. Hamid, The effect of adding Zn into the Sn-Ag-Cu solder on the intermetallic growth rate, *J. Mater. Sci. Mater. Electron.* 25 (7) (2014) 2913–2922, <https://doi.org/10.1007/s10854-014-1959-2>.
- [28] G. Zeng, S.D. McDonald, Q. Gu, Y. Terada, K. Uesugi, H. Yasuda, K. Nogita, The influence of Ni and Zn additions on microstructure and phase transformations in Sn-0.7Cu/Cu solder joints, *Acta Mater.* 83 (2015) 357–371, <https://doi.org/10.1016/j.actamat.2014.10.003>.
- [29] D.R. Frear, J.W. Jang, J.K. Lin, C. Zhang, Pb-free solders for flip-chip interconnects, *JOM* 53 (6) (2001) 28–33, <https://doi.org/10.1007/s11837-001-0099-3>.
- [30] C. Andersson, Z. Lai, J. Liu, H. Yu, Y. Jiang, Comparison of isothermal mechanical fatigue properties of lead-free solder joints and bulk solders, *Mater. Sci. Eng., A* 394 (1) (2005) 20–27, <https://doi.org/10.1016/j.msea.2004.10.043>.
- [31] A. Zoran Miric, A. Grusd, Lead-free alloys, *Solder. Surf. Mt. Technol.* 10 (1) (1998) 19–25, <https://doi.org/10.1108/09540919810203793>.
- [32] V.M.F. Marques, C. Johnston, P.S. Grant, Microstructural evolution at Cu/Sn-Ag-Cu/Cu and Cu/Sn-Ag-Cu/Ni-Au ball grid array interfaces during thermal ageing, *J. Alloys Compd.* 613 (2014) 387–394, <https://doi.org/10.1016/j.jallcom.2014.05.200>.
- [33] T. Xu, X. Hu, Y. Li, X. Jiang, The growth behavior of interfacial intermetallic compound between Sn-3.5Ag-0.5Cu solder and Cu substrate under different thermal-aged conditions, *J. Mater. Sci. Mater. Electron.* 28 (24) (2017) 18515–18528, <https://doi.org/10.1007/s10854-017-7799-0>.
- [34] P. Xue, S.-b. Xue, Y.-f. Shen, H. Zhu, Inhibiting the growth of Sn whisker in Sn-9Zn lead-free solder by Nd and Ga, *J. Mater. Sci. Mater. Electron.* 25 (6) (2014) 2671–2675, <https://doi.org/10.1007/s10854-014-1927-x>.
- [35] C.-W. Hwang, J.-G. Lee, K. Suganuma, H. Mori, Interfacial microstructure between Sn-3Ag-xBi alloy and Cu substrate with or without electrolytic Ni plating, *J. Electron. Mater.* 32 (2) (2003) 52–62, <https://doi.org/10.1007/s11664-003-0237-5>.